

Title : will be set by the publisher
Editors : will be set by the publisher
EAS Publications Series, Vol. ?, 2018

NON-LTE LINE FORMATION IN THE NEAR-IR: HOT STARS

Norbert Przybilla¹

Abstract. Line-formation calculations in the Rayleigh-Jeans tail of the spectral energy distribution are complicated by an amplification of non-LTE effects. For hot stars this can make quantitative modelling of spectral lines in the near-IR challenging. An introduction to the modelling problems is given and several examples in the context of near-IR line formation for hydrogen and helium are discussed.

1 Introduction

Near-infrared (near-IR) spectroscopy of early-type stars is a relatively new field. It is motivated by the desire to study early phases of massive star formation (when the stars are deeply embedded in their parental clouds) and to investigate young stellar populations throughout the Galactic disk and at the Galactic centre in particular. Despite hot stars showing a steep decline in flux levels towards longer wavelengths, observations in the near-IR become highly competitive with optical region spectroscopy for regions of high extinction. In some cases near-IR observations are the only means to penetrate the dust. The most prominent example is the Galactic centre, where the extinction in the K -band amounts to 3 mag, compared with more than 30 mag in V .

Near-IR spectroscopy became feasible only after substantial developments in detector technology over the past 15 years. Systematic observational studies of (normal) hot stars in the near-IR are nonetheless scarce. A spectral catalogue at low resolution ($R = \lambda/\Delta\lambda \lesssim 3000$) was compiled by Hanson et al. (1996) for OB-type stars. Classification spectra of early-type stars in the J , H and K bands can also be found in the atlases of Wallace & Hinkle (1997), Meyer et al. (1998) and Wallace et al. (2000). More recently, intermediate-resolution spectroscopy ($R \approx 10\,000$) became the standard (Fullerton & Najarro 1998; Hanson et al. 2005).

Unguided by observations, the field attracted little interest on the theoretical side, except for an early prediction of photospheric $\text{Br}\alpha$ emission in B-type stars

¹ Dr. Remeis-Sternwarte Bamberg & ECAP, Astronomisches Institut der Universität Erlangen-Nürnberg, Sternwartstrasse 7, D-96049 Bamberg, Germany

by Auer & Mihalas (1969a). Later, Zaal et al. (1999) could explain the observed emission cores of many near-IR hydrogen lines in early B-type stars via non-LTE effects, though several discrepancies between models and observation remained. The systematic behaviour of near-IR hydrogen and helium lines with spectral type and luminosity were investigated on theoretical grounds by Lenorzer et al. (2004) for O stars. Finally, the most comprehensive study of near-IR spectra of OB stars and a comparison with analyses in the optical was performed by Repolust et al. (2005).

Considerable work has also been done on the massive star population near the Galactic centre. For the most part, this comprises extreme stars like Luminous Blue Variables and Wolf-Rayet stars (e.g. Najarro et al. 1997, 2009; Martins et al. 2007). However, such objects are beyond the scope of the present discussion as their line spectra are formed in the stellar wind.

2 Challenges of non-LTE line-formation in the near-IR

The challenges of near-IR line formation in hot stars can be summarised in brief. Let us recall the expression for the line source function,

$$S_L = \frac{2h\nu^3/c^2}{(b_l/b_u)\exp(h\nu/kT) - 1}, \quad (2.1)$$

where b_l and b_u are the departure coefficients of the lower and upper level of the transition, respectively, ν is the transition frequency, T is the temperature and h , c and k are the Planck constant, the speed of light and the Boltzmann constant, respectively. The line source function is identical to the Planck function, B_ν , in LTE, i.e. deep in the stellar atmosphere ($b_l = b_u = 1$) or in cases where the lower and upper levels are tightly coupled ($b_l = b_u$). Spectral absorption lines experience non-LTE strengthening whenever $S_L/B_\nu < 1$ (for $b_l > b_u$), or they are weakened in the opposite case, potentially turning into emission lines when S_L exceeds the Planck function in the continuum.

The source function is particularly sensitive to variations in the ratio of the departure coefficients

$$|\Delta S_L| \underset{h\nu/kT \ll 1}{\approx} \left| \frac{S_L}{b_l/b_u - \exp(-h\nu/kT)} \Delta(b_l/b_u) \right| \quad (2.2)$$

when $h\nu/kT$ is small, i.e. in the Rayleigh-Jeans tail of the energy distribution. The denominator on the right hand side of Eqn. 2.2 can adopt values close to zero, amplifying effects of a varying $\Delta(b_l/b_u)$ considerably ('non-LTE amplification'). This can make near-IR lines in hot stars very susceptible to even small changes in the atomic data and details of the calculation. A quantitative reproduction of observed lines requires not only accurate knowledge of the plasma parameters (temperature and particle densities) and the radiation field in the stellar atmosphere, but also

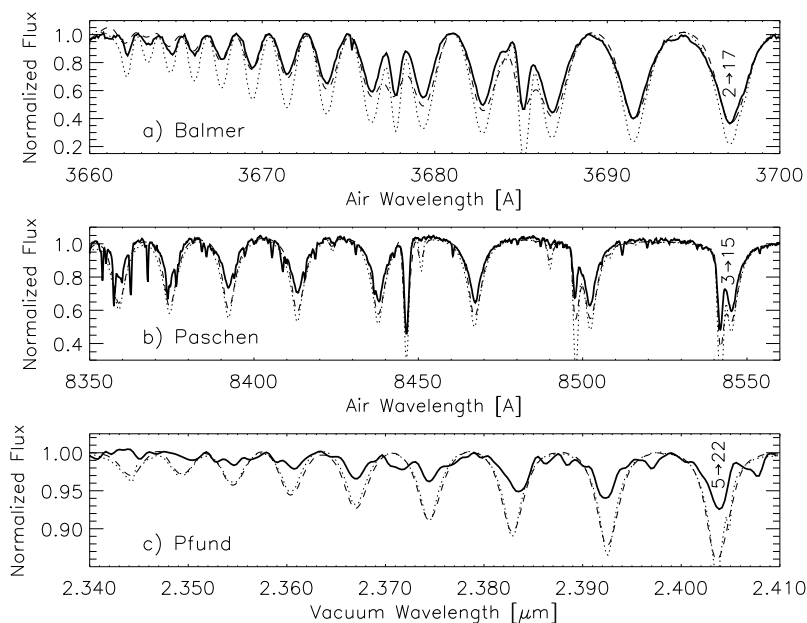


Fig. 1. Observed hydrogen lines (thick solid lines) from three series in Deneb (A2Ia): (a) Balmer, (b) Paschen, and (c) Pfund. Several strong metal lines are also present. The Paschen series is contaminated by many weak telluric features. Synthetic profiles from two model atmospheres are shown for comparison: a wind model (dashed line) and a hydrostatic model (dotted line). Note the discrepancies between observation and models in particular for the Pfund lines. From Aufdenberg et al. (2002), reproduced by permission of the AAS.

account for all relevant processes in model atoms and use of *high-precision atomic data* – even more so than required for analyses of hot star spectra in the visual region.

3 Applications

3.1 Hydrogen

The scope of problems with line-formation calculations in the near-IR can be exemplified with one of the brightest stars of the northern hemisphere, the A-supergiant prototype α Cyg (Deneb). Aufdenberg et al. (2002) encountered problems with the simultaneous non-LTE modelling of the Balmer and near-IR hydrogen lines (see Fig. 1), concluding, ‘These failures indicate that a spherically symmetric, expanding, steady state, line-blanketed, radiative equilibrium structure is not consistent with the conditions under which [...] the higher Pfund lines form.’ In the following we want to investigate whether a less drastic explanation can be found.

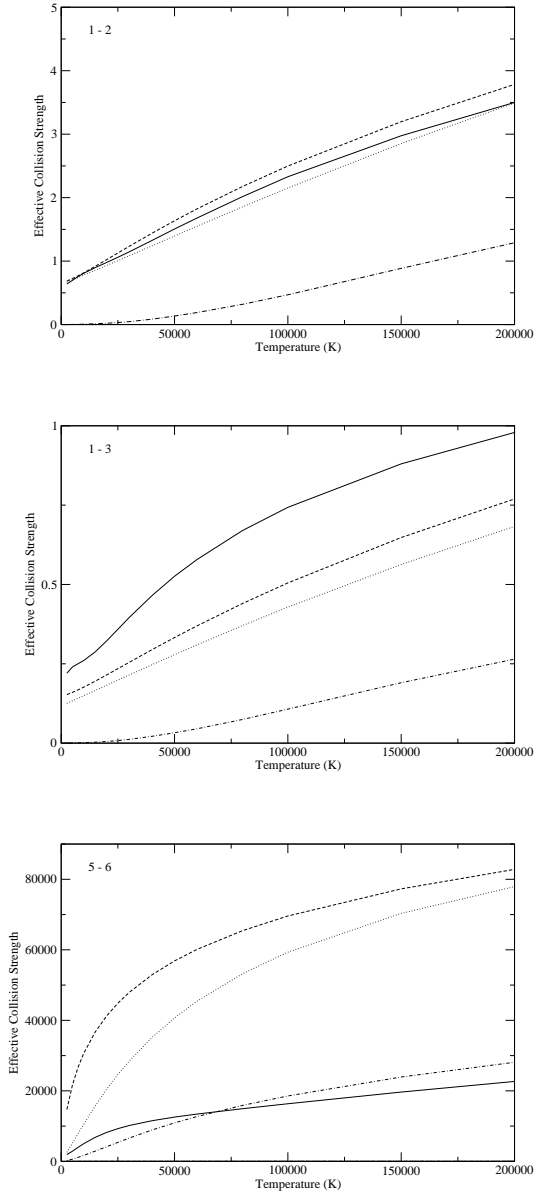


Fig. 2. Comparison of effective collision strengths in hydrogen for several transitions $n-n'$, as indicated. The curves are: Butler (as published in Przybilla & Butler 2004, solid line), Johnson (1972, dotted), Mihalas et al. (1975, dashed), Percival & Richards (1978, dash-dotted). From Przybilla & Butler (2004).

Table 1. Model Atom Implementations for H I

| Model | Electron-impact excitation data |
|-------|--|
| A | MHA (all n, n') |
| B | J72 (all n, n') |
| C | ABBS ($n, n' \leq 5$), MHA (rest) |
| D | ABBS ($n, n' \leq 5$), J72 (rest) |
| E | PB04 ($n, n' \leq 7$), PR ($n, n' \geq 5$), MHA (rest) |
| F | PB04 ($n, n' \leq 7$), PR ($n, n' \geq 5$), J72 (rest) |

ABBS: Anderson et al. (2000); J72: Johnson (1972); MHA: Mihalas et al. (1975); PB04: Przybilla & Butler (2004); PR: Percival & Richards (1978)

As explained above, small details *do* matter for line-formation calculations in the near-IR. The H I model atom used by Aufdenberg et al. looks reliable at first glance, given that 30 levels and over 400 transitions are accounted for explicitly in the non-LTE modelling. Moreover, the quantum-mechanical problem of the hydrogen atom can be solved analytically, such that the atomic data are of highest precision. But are they indeed?

The previous statement applies to radiative data. Hydrogen is exceptional as one important source of systematic uncertainty compromising studies of most ions of the other elements is thus excluded. However, collisions by electrons introduce a third particle to the Coulomb problem, such that *ab-initio* calculations are required to determine reliable cross-sections for collisional processes (excitation, ionization). Calculations of comprehensive sets of collisional data for all atomic levels of relevance in stellar atmospheres (lines up to $n \simeq 30$ may be observed in supergiants, see e.g. Fig. 1, while the Inglis-Teller limit is reached around $n \simeq 15$ to 20 for stars close to the main sequence) are still beyond present-day capabilities. However, it may be surprising to learn that reliable data for transitions involving levels of intermediate n were unavailable for a long time.

In the absence of reliable data one has to resort to approximations. Approximation formulae are based on simplifying theoretical considerations and indirect experimental evidence (see e.g. discussion by Mihalas 1967). As a boundary condition they should reproduce experimental constraints in the few cases where such are available. The approximations should provide data accurate to a factor better than two, and some studies claim the uncertainties to be as small as $\sim 20\%$.

A comparison of various approximation formulae with *ab-initio* data for effective collision strengths for electron-impact excitation of several transitions having initial/final quantum numbers n, n' in neutral hydrogen is shown in Fig. 2. Good agreement is found between the frequently-used approximations according to Johnson (1972) and Mihalas et al. (1975) with recent *ab-initio* data for the Ly α transition (1–2), as expected. The semi-empirical results of Percival & Richards (1978) are displayed in this case for completeness only, as they are valid for $n, n' \geq 5$. The comparison for transitions with higher n, n' shows that uncertainty estimates for some approximations may be too optimistic.

The question of which data should be preferred for non-LTE model atoms has to be answered by comparison with observation. Przybilla & Butler (2004) con-

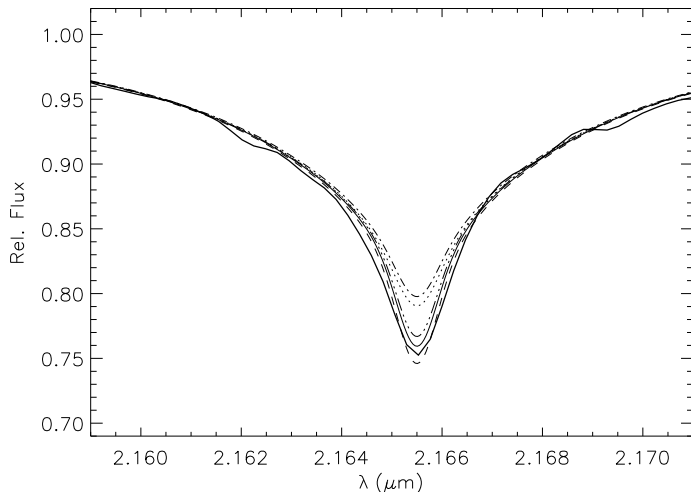


Fig. 3. Spectrum synthesis for $\text{Br}\gamma$ in Vega (A0 V): models A, C, E and F (dotted, dash-dot-dot-dotted, full, dashed lines) and an LTE profile (dashed-dotted) are compared with observation (thick full line). Models B and D are omitted for clarity as they are almost identical to model F. From Przybilla & Butler (2004).

structured several HI model atoms for this task (see Table 1 for a selection of data used for the evaluation of collisional excitation rates). Coverage of a wide range of plasma parameters for the tests is essential for the comparison, therefore, main sequence and supergiant stars of spectral types A, B and O were investigated. Stellar parameters were adopted from earlier detailed studies of their optical spectra. Note that the model atoms from Table 1 give almost indistinguishable profiles for the lines of the Balmer series. A few examples from the comparison are now provided.

The A0 V star Vega is one of the most intensely studied stars, and in most respects well described by the assumption of LTE. The Balmer and Paschen lines are, in general, well matched by LTE computations, and these are practically identical to non-LTE results. However, comparison with the observed $\text{Br}\gamma$ profile in Fig. 3 shows that LTE modelling fails to reproduce the line core, predicting a too shallow core. Non-LTE computations can improve on this, except for model A, which differs only slightly from LTE. Model A can therefore be disregarded for all other comparisons. However, on the basis of this one case alone a decision as to which of the model atoms B through F should be favoured cannot be drawn, as despite being noticeable the differences between these models are not highly significant.

Non-LTE effects become stronger in supergiants, such that differences in the predictions from different model atoms can be expected to be amplified as well. Comparisons of predictions for Br10 and Br11 (which are of photospheric origin,

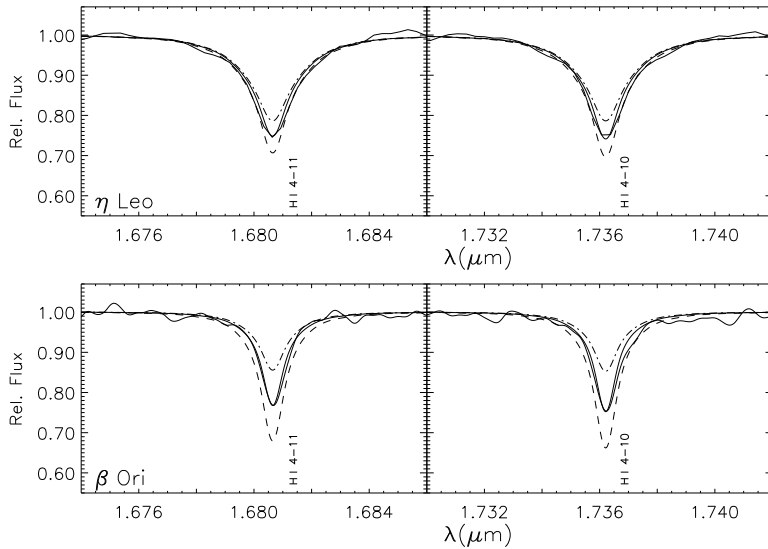


Fig. 4. Higher Brackett lines in η Leo (A0 Ib) and β Ori (B8 Ia): models E (full lines), F (dashed) and LTE calculations (dashed-dotted) are compared with observation (thick full). Profiles from models B and D resemble the model F predictions and are not shown here. Model C gives a slightly less good fit than model E. From Przybilla & Butler (2004).

unaffected by the stellar wind) in the supergiants η Leo (A0 Ib) and β Ori (B8 Ia) are shown in Fig. 4. Indeed, all models using the Johnson’s (1972) approximation formula (B, D and F) can be discarded as they produce too deep line cores. Equivalent widths are predicted too strong, by about a factor 2 in the more luminous supergiant β Ori (LTE equivalent widths are too low by about the same factor). The remaining two models, C and E, produce similar predictions, with model E providing a slightly better fit to the observation, thus it becomes the recommended model for further use. The whole comparison process was more complicated than sketched here, involving more stars and more lines of the Balmer, Paschen, Brackett and Pfund series. Full details can be found in Przybilla & Butler (2004).

The mechanisms driving departures of hydrogen from detailed balance in the atmospheres of early-type stars seemed to be well understood since the seminal work of Auer & Mihalas (1969b, 1969c), and numerous subsequent contributions – for line formation in the IR e.g. by Zaal et al. (1999). Indeed, various choices of the (mostly approximate) collisional data produce no significant differences in the stellar continuum or the Balmer line profiles, i.e. the features that are the starting point for quantitative analyses using model atmosphere techniques. On the other hand, the *local* processes that *modify* the radiatively induced departures from LTE become a dominant factor for line-formation computations in the IR.

The example of β Ori is used to deepen the discussion. Departure coefficients $b_i = n_i/n_i^*$ (the n_i and n_i^* being the non-LTE and LTE populations of level i , respectively) for selected levels in calculations using models A–F are displayed in

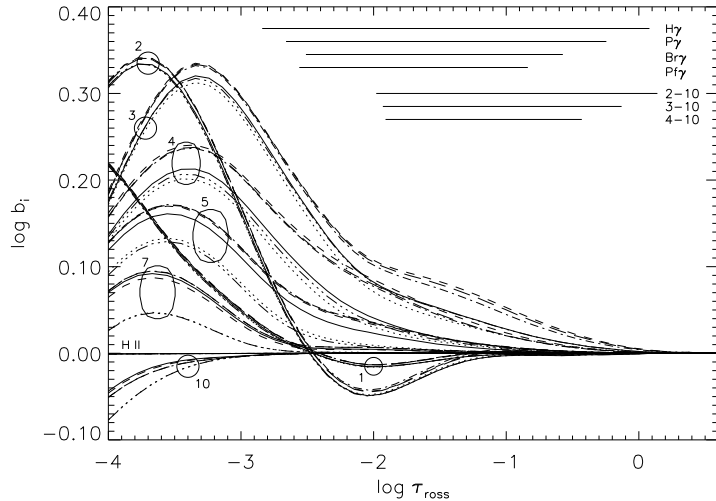


Fig. 5. Run of departure coefficients b_i in β Ori as a function of Rosseland optical depth, τ_{ross} , models A through F (dotted, dashed-dotted, dash-dot-dot-dotted, long dashed, full, dashed lines). The individual sets of graphs are labelled according to the levels' principal quantum number; all graphs for H II coincide. Line-formation depths (core to wing) for a few features are indicated. From Przybilla & Butler (2004).

Fig. 5. The overall behaviour, i.e. the over- and under-population of the levels of the minor ionic species and the major species H II, is governed by the radiative processes, while the differences in the collisional data lead to modulations. These are very small for the ground state and become only slightly more pronounced for the $n=2$ level, as these are separated by comparatively large energy gaps from the rest of the term structure. Only colliding particles in the high-energy tail of the Maxwell distribution are able to overcome these energy differences at the temperatures in the stellar atmosphere. Thus, computations of the model atmosphere structure will not be significantly influenced, as the important bound-free opacities of hydrogen vary only in a negligible way. The IR line formation will be affected, as maximum effects from variations of the collisional data are found for the levels with intermediate n at line-formation depth.

In fact, the differences in the collisional cross-sections from approximation formulae and *ab-initio* computations are largest for transitions among the $n=3-7$ levels with $\Delta n=1$ and 2, and they can amount to more than an order of magnitude. The higher Rydberg states show less sensitivity as they approach the limiting case of LTE, which is independent of the details of individual (de-)populating mechanisms. Collisional cross-sections from *ab-initio* computations up to $n \simeq 7$ are therefore sufficient to eliminate a significant source of systematic error. Using the available data it turns out that the MHA- (models A, C, E) and J72-type approximations (models B, D, F) give rise to basically two sets of distinct be-

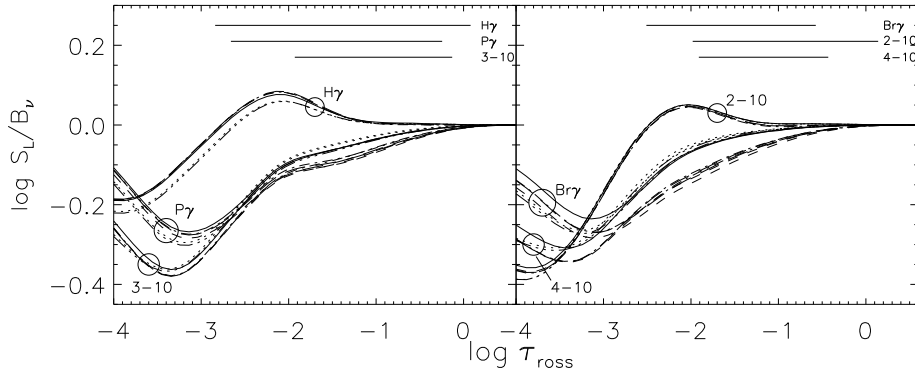


Fig. 6. Ratio of line source function S_L to Planck function B_ν at line centre as a function of τ_{cross} in β Ori. Line designations as in Fig. 5. From Przybilla & Butler (2004).

haviour, with the former tending to dampen non-LTE departures more efficiently than the latter, due to larger collisional cross-sections. Such differences in the level populations are the cause for the line-profile variations as in Figs. 3 and 4. In fact, the b_i typically vary by only several percent, but non-LTE amplification changes equivalent widths by a factor ~ 2 in the example shown in Fig. 4. The corresponding reaction of the line-source function to variations in the collisional data is displayed in Fig. 6.

Finally, we may ask how the comparison of spectrum synthesis based on the recommended model atom E looks like for Deneb, the starting point of our discussion. Indeed, an excellent match of model and observation can be obtained, as shown by Schiller & Przybilla (2008), see Fig. 7. Note that the lower members of the Balmer, Paschen and Brackett series are affected by the stellar wind of this supergiant. Consequently, computations based on the hydrodynamic non-LTE code FASTWIND are shown for the comparison in this case, while hydrostatic calculations with DETAIL/SURFACE based on an ATLAS9 atmosphere are sufficient for the lines of photospheric origin.

3.2 Helium

As in the case of hydrogen, non-LTE effects on He I lines are stronger in the near-IR than in the optical. An example for the (relatively weak) $\lambda 2.11 \mu\text{m}$ singlet and triplet feature in the K -band spectrum of τ Sco (B0.2 V) is shown in Fig. 8. These lines experience a very pronounced non-LTE strengthening. The stellar parameters for the calculations were determined by analysis of the optical spectrum.

Details of the model atom and of the modelling assumptions also play an important rôle for non-LTE line-formation computations for He I in the near-IR. Considerable differences exist between photoionization cross-sections used in classical studies of He I line formation in early B-type stars and modern *ab-initio* data. A comparison of the data for the metastable $2s^3S$ state (the lower level of the He I 10830 Å transition) is shown in Fig. 9, displaying results of Gingerich (1964)

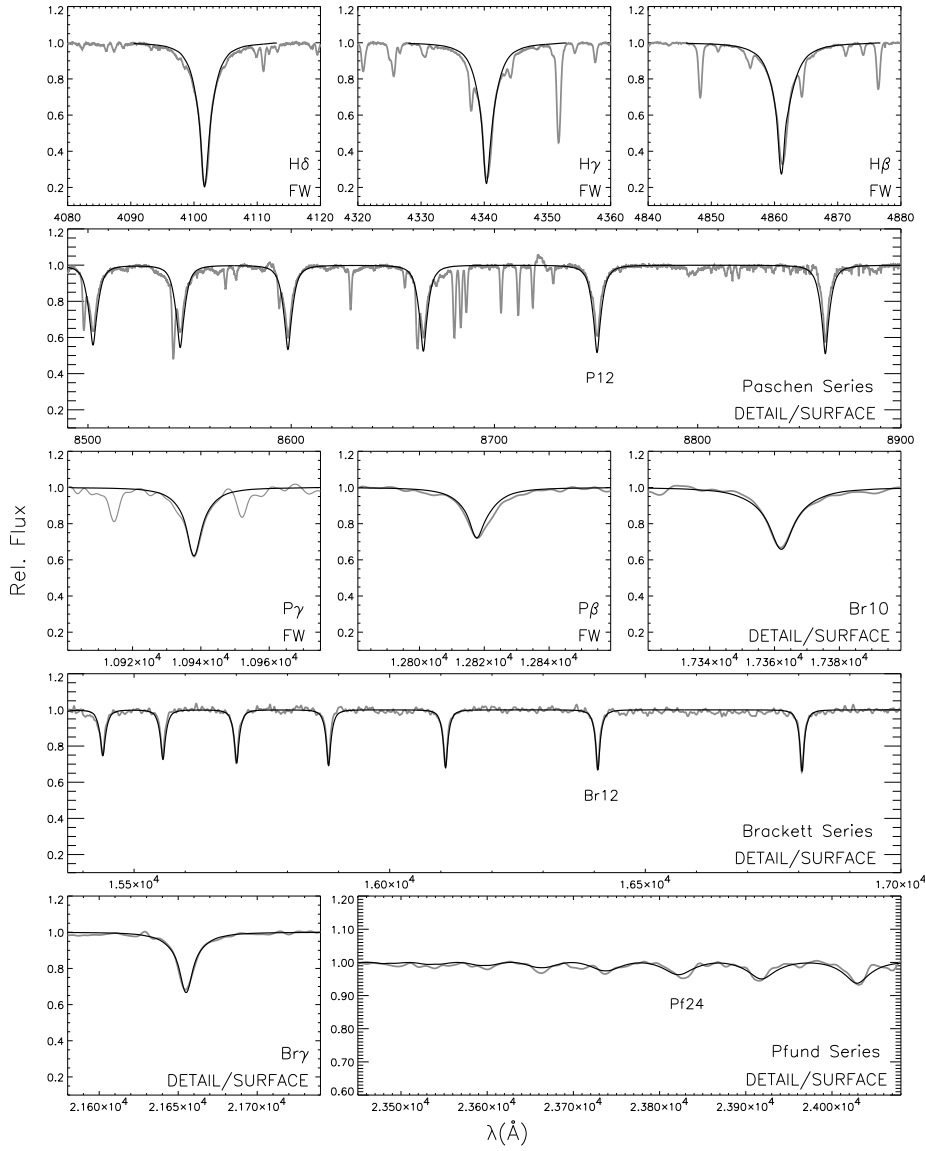


Fig. 7. Modelling (black) of the hydrogen lines in the visual and the near-IR spectrum of Deneb (gray curve). Overall, a good to excellent agreement is achieved, compare with Fig. 1. The synthetic spectra are calculated with a hybrid non-LTE technique using DETAIL/SURFACE (photospheric lines) or FASTWIND (FW, wind-affected lines), as indicated. Except for the Pfund series, all panels show the same range in relative flux. Some lines, such as $P\beta$ and $H\beta$, are noticeably affected by the stellar wind. According to Schiller & Przybilla (2008).

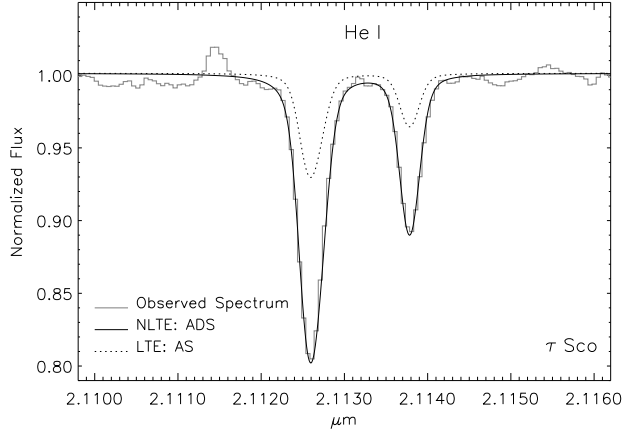


Fig. 8. Modelling of the He I $\lambda 2.11 \mu\text{m}$ singlet and triplet feature (*K*-band) in τ Sco (B0.2 V). Like in the case of hydrogen, near-IR transitions of He I experience, in general, stronger non-LTE effects than the lines in the visual. From Nieva & Przybilla (2007).

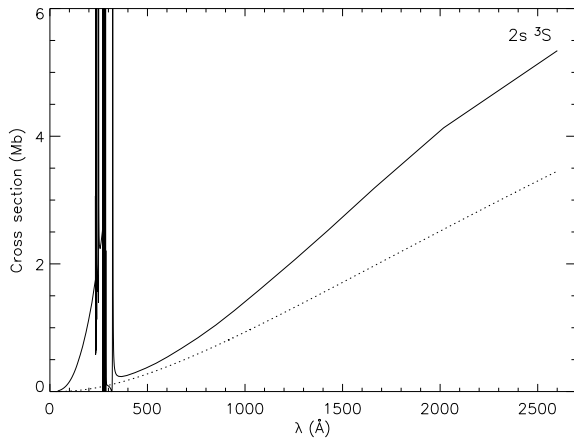


Fig. 9. Comparison of the photoionization cross-sections for the He I $2s \ ^3S$ state (Fernley et al. 1987, full line), as used in our reference He I model atom, and of Gingerich (1964, dotted), as used in previous model atoms by Auer & Mihalas (1973) and Husfeld et al. (1989). The cross-sections differ by more than 50% at threshold. From Przybilla (2005).

and of Fernley et al. (1987), as obtained within the Opacity Project. The modern data give a cross-section at threshold larger by more than 50%. Note that the presence of the resonance structure at short wavelengths is irrelevant for the problem, as the stellar flux is negligible there, resulting in an insignificant contribution to the photoionization rate.

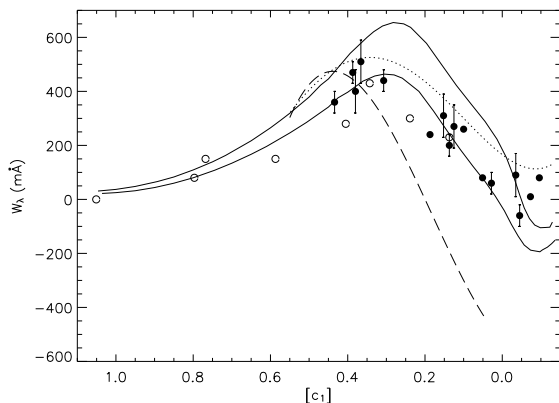


Fig. 10. Comparison of observed equivalent widths for He I 10 830 Å in B-type stars (Lennon & Dufton 1989: filled circles; Leone et al. 1995: open circles) with model predictions: Auer & Mihalas (1973, dotted line), Dufton & McKeith (1980, dashed line), and our own calculations (full lines) for microturbulence $\xi = 0$ (lower) and 8 km s^{-1} (upper curve). The abscissa is the reddening-free $[c_1]$ index, a temperature indicator, spanning a range from early A to late O. From Przybilla (2005).

The too low cross-sections were already corrected in calculations by Dufton & McKeith (1980), leading to predictions of strong emission for He I 10 830 Å in early B-type stars in contrast to absorption predicted by Auer & Mihalas (1973) using the Gingerich (1964) data. Surprisingly, observations by Lennon & Dufton (1989) favoured the predictions made with the incorrect data, at least qualitatively, as the line was found to be in absorption in most cases (Fig. 10). A satisfactory reproduction of the observed trend was also not obtained later by Leone et al. (1995). Shortcomings in the model atmospheres were invoked in both cases.

Again, a small detail of the calculations has a large effect on the predicted line profile. Good agreement between the observed trend and model calculations for the near-IR line He I 10 830 Å was finally obtained by Przybilla (2005), using modern atomic data and accounting for *line-blocking effects* in the non-LTE computations, see Fig. 10. It turns out that the traditionally analysed He I lines in the optical region are not very sensitive to whether line blocking is accounted for or not.

The effects of using photoionization cross-sections from Gingerich (1964, as implemented in the He I model atom of Husfeld et al. 1989) and of Fernley et al. (1987, as implemented in the reference model by Przybilla 2005) on departure coefficients of the $n = 1$ and 2 levels are shown in Fig. 11. Only the departure coefficients for the $2s^3S$ state show differences of as little as $\sim 5\%$ at line-formation depths, i.e. only the He I 10 830 Å transition is affected – $2p^1P^o$ and $2p^3P^o$ are the lower levels of the He I lines in the optical region. Note that as a consequence line-formation depths also change. Almost the entire effect can be accounted for by the $2s^3S$ photoionization cross-section. Practically all other differences between the two sets of data are negligible for the problem.

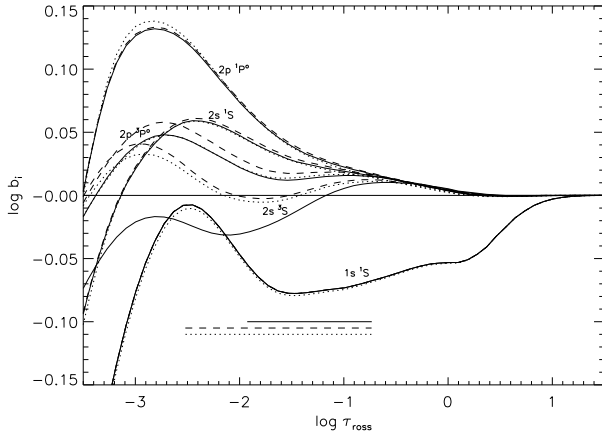


Fig. 11. Comparison of departure coefficients b_i as a function of τ_{ross} for the $n=1$ and 2 levels of He I from computations using the Husfeld et al. (1989, dotted lines) and our reference model atom (full lines), and computations for this new model atom with the photoionization cross-section for the $2s^3S$ state replaced by that used in the older one (dashed lines). Line-formation depths for He I $\lambda 10830 \text{ \AA}$ are indicated. The computations are for a stellar atmospheric model with $T_{\text{eff}} = 30\,000 \text{ K}$, $\log g = 4.0$ (cgs), $\xi = 0 \text{ km s}^{-1}$, solar metallicity, and solar helium abundance. From Przybilla (2005).

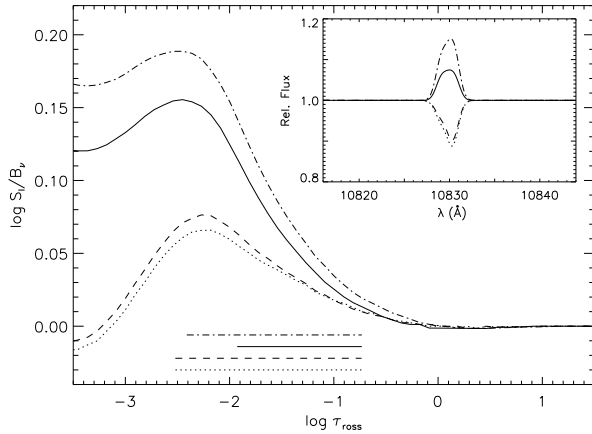


Fig. 12. Ratio of S_L to B_ν at the centre of the 10830.34 \AA fine-structure component of the transition for the same atmospheric parameters as in Fig. 11. In addition to line designations from Fig. 11, the dashed-dotted line shows results from a computation using the new model atom, but neglecting line blocking. In the inset the resulting line profiles are compared after convolution with a Gaussian of FWHM of 20 km s^{-1} . Use of the improved photoionization cross-sections turns the absorption into emission, while neglect of line blocking gives excess emission. From Przybilla (2005).

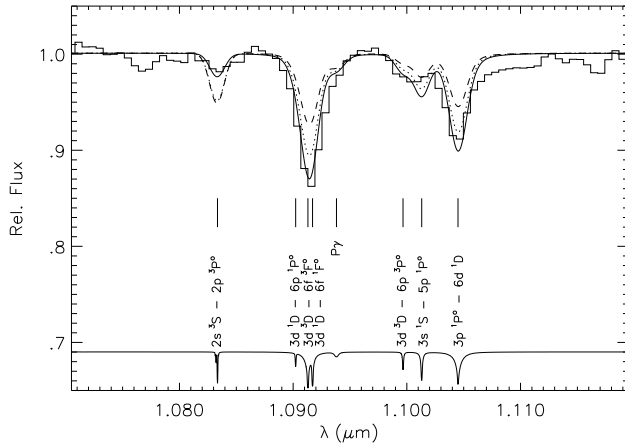


Fig. 13. Comparison of the normalised J -band spectrum of the extreme helium star V652 Her (histogram) in the region around He I $\lambda 10830 \text{ \AA}$ with three model predictions: LTE (dashed line) and two non-LTE computations using the model atom of Husfeld et al. (1989, dotted line) and the improved model atom of Przybilla (2005, full line). In contrast to the other transitions, He I $\lambda 10830 \text{ \AA}$ experiences strong non-LTE weakening. An unbroadened synthetic spectrum is displayed at the bottom in order to illustrate what can be expected from high-resolution observation. From Przybilla et al (2005).

The response of the line source function to photoionization cross sections is shown in Fig. 12. Non-LTE calculations based on the (incorrect) older photoionization data yield absorption lines that are shallower than in LTE. Computations based on modern cross-sections give weak emission, while neglect of line blocking results in excess emission. Finally, the predicted trends discussed in the literature are thus understood.

He I 10830 \AA is not the only near-IR line of neutral helium that is sensitive to non-LTE amplification. A comparison of the observed spectrum of the extreme helium star V652 Her in the J -band with synthetic spectra for two different model atoms (and an LTE calculation) shows that all lines are affected (Przybilla et al. 2005). Our reference model atom succeeds in reproducing all the lines simultaneously. While He I 10830 \AA experiences non-LTE weakening, the other features are subject to non-LTE strengthening.

4 Conclusions & Outlook

We have seen that amplification of non-LTE effects is ubiquitous for near-IR lines in hot stars. This makes non-LTE line-formation calculations challenging, as every aspect of the modelling has to be considered properly. On the other hand, the high sensitivity offers the possibility to put tight constraints on the atomic data selected for the construction of non-LTE model atoms. Deficits in the data will show up in the comparison of the model predictions with observation.

The near-IR studies of hot stars so far comprise relatively strong lines of hydrogen and helium, based on medium-resolution spectra. The new generation of high-resolution near-IR spectrographs like CRIRES on the VLT promise to revolutionise the field. In particular, a multitude of (weak) metal lines will become accessible for the first time (see e.g. Przybilla et al. 2009; Nieva et al. 2009). The development of proper non-LTE models will turn quantitative near-IR spectroscopy of hot stars into a crucial tool for Galactic studies, and with the upcoming extremely large telescopes (diffraction-limited observations using adaptive optics will be feasible only at near-IR wavelengths) also for extragalactic stellar astronomy.

References

- Anderson, H., Ballance, C. P., Badnell, N. R. & Summers, H. 2000, *J. Phys. B*, 33, 1255
- Auer, L. H. & Mihalas, D. 1969a, *ApJ*, 156, L151
- Auer, L. H. & Mihalas, D. 1969b, *ApJ*, 156, 157
- Auer, L. H. & Mihalas, D. 1969c, *ApJ*, 156, 681
- Auer, L. H. & Mihalas, D. 1973, *ApJS*, 25, 433
- Aufdenberg, J. P., Hauschildt, P. H., Baron, E., et al. 2002, *ApJ*, 570, 344
- Dufton, P. L. & McKeith, C. D. 1980, *A&A*, 81, 8
- Fernley, J. A., Taylor K. T. & Seaton M. J. 1987, *J. Phys. B*, 20, 6457
- Fullerton, A. W. & Najarro, F. 1998, in: *“Boulder-Munich II: Properties of Hot, Luminous Stars”*, ed. I. D. Howarth (ASP: San Francisco), p. 47
- Gingerich, O. 1964, in *“Proceedings of the First Harvard-Smithsonian Conference on Stellar Atmospheres”*, ed. E. H. Avrett, O. J. Gingerich & C. A. Whitney, SAO Spec. Rep. 167 (Cambridge: SAO), 17
- Hanson, M. M., Conti, P. S. & Rieke, M. J. 1996, *ApJS*, 107, 311
- Hanson, M. M., Kudritzki, R. P., Kenworthy, M. A., et al. 2005, *ApJS*, 161, 154
- Husfeld, D., Butler, K., Heber, U. & Drilling, J. S. 1989, *A&A*, 222, 150
- Johnson, L. C. 1972, *ApJ*, 174, 227
- Lennon, D. J. & Dufton, P. L. 1989, *A&A*, 225, 439
- Lenorzer, A., Mokiem, M. R., de Koter, A. & Puls, J. 2004, *A&A*, 422, 275
- Leone, F. & Lanzafame, A. C. 1998, *A&A*, 330, 306
- Leone, F., Lanzafame, A. C. & Pasquini, L. 1995, *A&A*, 293, 457
- Martins, F., Genzel, R., Hillier, D. J., et al. 2007, *A&A*, 468, 233
- Meyer, M. R., Edwards, S., Hinkle, K. H. & Strom, S. E. 1998, *ApJ*, 508, 397
- Mihalas, D. *ApJ*, 149, 169
- Mihalas, D., Heasley, J. N. & Auer, L. H. 1975, *A Non-LTE Model Stellar Atmospheres Computer Program*, NCAR-TN/STR 104
- Najarro, F., Krabbe, A., Genzel, R., et al. 1997, *A&A*, 325, 700
- Najarro, F., Figer, D. F., Hillier, D. J., et al. 2009, *ApJ*, 691, 1816
- Nieva, M. F. & Przybilla, N. 2007, *A&A*, 467, 295
- Nieva, M. F., Przybilla, N., Seifahrt, A., et al. 2009, in *“Science with the VLT in the ELT era”*, ed. A. Moorwood (Springer: Berlin), p. 499

- Percival, I. C. & Richards, D. 1978, MNRAS, 183, 329
- Przybilla, N. 2005, A&A, 443, 293
- Przybilla, N. & Butler, K. 2004, ApJ, 609, 1181
- Przybilla, N., Butler, K., Heber, U. & Jeffery, C. S. 2005, A&A, 443, L25
- Przybilla, N., Seifahrt, A., Butler, K., et al. 2009, in “*Science with the VLT in the ELT era*”, ed. A. Moorwood (Springer: Berlin), p. 55
- Repolust, T., Puls, J., Hanson, M. M., et al. 2005, A&A, 440, 261
- Schiller, F. & Przybilla, N. 2008, A&A, 479, 849
- Wallace, L. & Hinkle, K. 1997, ApJS, 111, 445
- Wallace, L., Meyer, M. R., Hinkle, K. & Edwards, S. 2000, ApJ, 535, 325
- Zaal, P. A., de Koter, A., Waters, L. B. F. M., et al. 1999, A&A, 349, 573